14th International Conference on Structural Safety and Reliability - ICOSSAR'25
1-6 June, 2025 - Los Angeles California, USA
R. Ghanem, E. Johnson, S. Masri and A. Olivier (Eds)

DEVELOPMENT OF A PROBABILISTIC FINITE ELEMENT MODEL FOR THE VALIDATION OF STRUT-AND-TIE MODELS IN HALF-JOINT GIRDERS

KITO LUYTEN[1], WOUTER BOTTE[2] AND ROBBY CASPEELE[3]

[1, 2, 3] Department of Structural Engineering and Building Materials, Laboratory Magnel-Vandepitte for Concrete Research, Ghent University
Tech Lane Ghent Science Park, 9052 Ghent, Belgium
[1]kito.luyten@ugent.be, [2]wouter.botte@ugent.be, [3]robby.caspeele@ugent.be

Key words: Half-joint, FEM, Strut-and-tie model, Uncertainty quantification.

Abstract. Discontinuity regions in concrete structures, such as half-joints, exhibit complex stress distributions that challenge traditional design approaches. This study presents a probabilistic assessment of the structural capacity of a concrete half-joint by comparing strut-and-tie models (STMs) with detailed finite element models (FEMs), taking into account parameter uncertainties. A validated 3D FEM is employed as a benchmark to evaluate the conservative nature of the STM and to compare the reliability index and failure probability. These are calculated using Latin Hypercube sampling in combination with the FEM simulations or the STMs and the first-order reliability method (FORM) and by using the FORM directly in combination with the STMs. Results show that the STM provides a safe lower bound estimate of capacity, but with some margin for improvement, particularly if the models are applied for assessment situations. A significant overexceedance of the probabilistically calculated reliability index with respect to its target design value and the corresponding conservativeness of the designed structure is observed. Further, distinct failure mechanisms observed in the FEM simulations highlight the limitations of STMs in capturing post-yield behaviour and load redistribution. This work underscores the potential of probabilistic FEMs as a validation tool for the calibration of simplified STM-based approaches and stresses the advantages and shortcomings of the current state-of-the art application of these approaches.

1 INTRODUCTION

Discontinuity regions in concrete structures, such as half-joints, present significant challenges in structural design due to their complex stress distributions and localised effects. For such regions, strut-and-tie models (STMs) provide a practical and simplified method for estimating the load-carrying capacity, making them valuable tools in engineering practice. However, since STMs are inherently conservative and represent a lower bound of the actual capacity, there is a need to validate the accuracy of STMs against more detailed numerical models, in order to arrive at a more performance-based design or to enable adequate assessment.

Finite element models (FEMs) offer a powerful means to perform this validation, enabling a direct comparison between the simplified STM predictions and more realistic simulations of structural behaviour. It allows a one-to-one evaluation to assess whether this lower bound sufficiently approximates the actual capacity and captures the failure behaviour.

In addition, it is important to recognise that structural behaviour in discontinuity regions is influenced by several uncertainties, including material properties and even time-dependent degradation due to corrosion, all influencing the dominant failure mechanism that can materialise. To account for the realistic effects of these uncertainties, a probabilistic FEM approach is essential. It enables not only the validation of STM predictions under uncertainty but also the quantification of the distribution of the structural capacity, the failure probability and the associated reliability index.

This study focuses on bridging the gap between idealised STM formulations and realistic structural behaviour through probabilistic FEMs, providing deeper insight into the reliability and safety of structures with discontinuity regions.

2 CASE STUDY

2.1 Structural layout

In this contribution, a case study is used to compare strut-and-tie models to finite element models, with and without considering the influence of parameter uncertainties. It concerns a half-joint girder subjected to a centrally applied point load based on the concrete specimens described in [1] and [2]. The considered beam has a width b of 400 mm, a height h of 700 mm, and a length l of 3140 mm, measured between the supports. The concrete cover c is 40 mm, the nib's height h_n is 325 mm, and its length l_n is 260 mm. A steel plate supports the nib and has dimensions 400 mm × 140 mm × 30 mm. The reinforcement layout, shown in Figure 1, includes: 5 ϕ25 bars as bottom reinforcement, 5 ϕ20 bars as top reinforcement, 3 ϕ12 U-bars, 4 ϕ10 double-legged stirrups near the nib, 5 ϕ10 triple-legged stirrups near the mid span and 4 ϕ12 diagonal bars [1] [2].

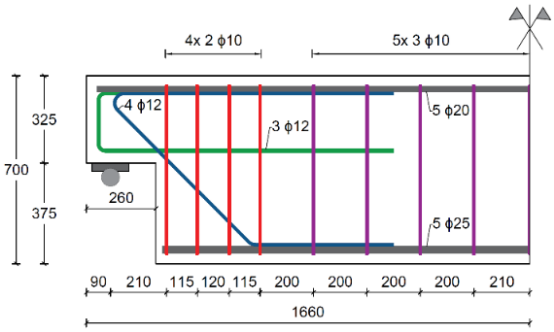

Figure 1: Reinforcement – Case study (dimensions in mm)

2.2 Finite element model

For this contribution, a finite element model (FEM) is created in the software Abaqus to act as a benchmark for the lower bound strut-and-tie model calculations. The mesh size is 50 mm. The 3D model uses 8-node linear hexagonal brick elements with reduced integration (C3D8R) for the concrete and 2-node linear beam elements for the reinforcement. For the equivalent 2D model, on the other hand, 4-node bilinear plane strain quadrilateral elements with reduced integration (CPE4R) are used for the concrete and 2-node linear truss elements for the reinforcement. The use of truss elements reduces the calculation time in comparison to beam

elements since these can only be loaded in compression or tension and not in bending. Further, in the 2D model, the different out-of-plane rebars and the double and triple-legged stirrups are lumped as one rebar with an equivalent cross-section.

The material model for concrete in compression is based on EN 1992-1-2, and for the tensile behaviour, Hordijk's curve is applied to relate the crack width to the acting stress. The concrete class is C30/37. A simple bi-linear diagram is used to model the steel behaviour of class S500.

There is chosen for a displacement-controlled calculation of the FEM instead of a load-controlled calculation as the latter is unable to represent the softening, post-peak behaviour of the structure.

2.2.1 Improving calculation efficiency

As the goal of this contribution is to perform probabilistic calculations with the developed FEM, it is crucial to reduce its required calculation time.

The calculation efficiency can be improved within one FEM by running the calculation in parallel. In this case, MPI processing was used.

Further, the efficiency can also be increased by shifting from a 3D to a 2D model. This possibility can be considered because of the regular layout and loading of the case study. Additionally, the stresses in the rebars that are lumped when changing from a 3D to a 2D model are approximately the same. Finally, the sampling method is another important aspect to consider in order to improve the calculation efficiency. By using Latin Hypercube sampling to determine the probability density function of the resistance in combination with the first-order reliability method to determine the failure probability P_f and reliability index β taking into account the uncertainties related to the loads and model uncertainties, the calculation efficiency is strongly improved in contrast to using inefficient Monte Carlo sampling, for which an amount of samples, and hence FEM calculations, in the order of magnitude 10^6 are required to achieve accurate estimations of P_f and β. However, there are also other efficient variance-reducing methods such as response surface modelling. Applying these holds the potential to further increase the calculation efficiency.

2.2.2 Validation of the developed FEMs

Based on the experimental data from the research of Desnerck et al. [1] [2] the FEMs are validated for their correctness and accuracy. The concrete strength and steel strengths reported in the references are adopted in the FEMs' material models. The resulting load-deflection curves of the displacement-controlled calculation are shown in Figure 2. As can be seen, the FEM output matches the experimental curve very well. There is a slight overestimation of the initial cracking moment, which could be related to the formulation used for the fracture energy of concrete. In this contribution, the formulation of the *fib* Model Code 2020 is used with $f_{ck} = f_{cm} - 8$:

$$G_f = 85\, f_{ck}^{0.15} \tag{1}$$

Further, the calculated peak loads of 392.9 kN and 394.3 kN for the 3D and 2D models, respectively, approach the experimentally measured value of 402.3 kN, and all values correspond to a mid-span deflection of around 10 mm. The experiment is considered to have failed just after this peak load, as it was a load-controlled set-up, while the FE analyses retain

some residual capacity afterwards due to their displacement-controlled behaviour. The main drop in capacity occurs when the ultimate strength of the diagonal reinforcement bars is reached, i.e. corresponding to the ultimate strain. The observed failure mechanism in the FEM simulations is compatible with the performed experiment.

In conclusion, the results of the 3D FEM lie very close to the performed experiment and hence this FEM can be considered as validated and can be used as a benchmark for the validation of the STMs in a probabilistic manner. Also the 2D FEM curve approximates the experimental curve well and is hence a sufficiently accurate alternative to the 3D model with a much shorter calculation time.

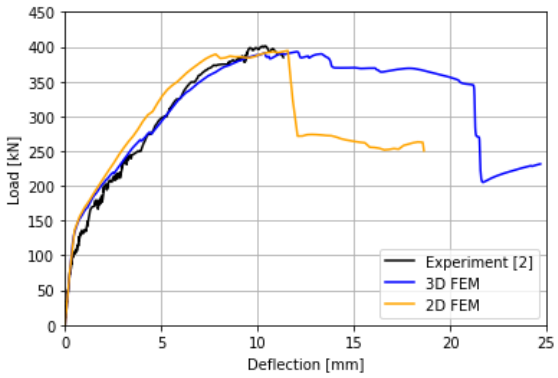

Figure 2: Load-deflection curve

2.3 Strut-and-tie model

The structural capacity and safety of a concrete half-joint can be assessed using a strut-and-tie model (STM). As STMs are applications of the static method of limit analysis, which provides a lower bound for the structural capacity, there is no single correct STM [3]. The most representative STM for the given reinforcement layout in Figure 1 incorporates both the orthogonal reinforcement and diagonal reinforcement, and is shown in Figure 3.

For a comprehensive explanation of the stress calculations and resistance determinations within this STM, readers are referred to Luyten et al. [4], Desnerck et al. [1] and EN 1992-1-1 [5].

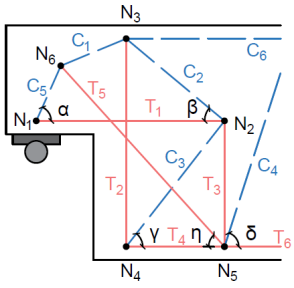

Figure 3: Applied STM (C designates a compression strut, T designates a tension tie)

3 PROBABILISTIC CALCULATIONS OF THE FAILURE PROBABILITY

3.1 Characteristics of the stochastic variables

The input parameters for the probabilistic calculations and their stochastic distributions are listed in Table 1 and follow the recommendations of the Probabilistic Model Code of JCSS [6]. The loads and material strengths are probabilistic variables. Dimensions and reinforcement areas are treated as deterministic. The reference period for the imposed variable load is 50 years.

Table 1: Stochastic input parameters

Parameter	Distribution	Characteristic (X_k)	Mean (μ)	COV (δ)	Reference
Permanent load, G [kN]	Normal	109	109 ($G_m = G_k$)	0.10	[7]
Variable load (t_{ref} = 50 years), Q_{50} [kN]	Gumbel	73	44 ($Q_m = 0.6 \cdot Q_k$)	0.35	[7]
Concrete strength, f_c [MPa]	Lognormal	30	38 ($f_{cm} = f_{ck} + 8$)	0.15	[7]
Steel yield strength, f_y [MPa]	Lognormal	500	560 ($f_{ym} = f_{yk} + 60$)	0.054	[7]
Young's modulus of steel, E_s [MPa]	Deterministic	-	210 000	-	-
Resistance model uncertainty, K_R [-]	Lognormal	-	1.2	0.15	[7]
Load model uncertainty, K_E [-]	Lognormal	-	1.0	0.10	[7]

To determine the design load E_d, the design resistance R_d of the half-joint is first calculated based on the STM using the partial factors from the Eurocode for a reference period t_{ref} of 50 years and a target reliability index β_{target} of 3.8. The design load and resistance are related as shown in Eq. (2).

$$E_d\,(G_d, Q_d) = R_d\,(f_{cd}, f_{yd}) \tag{2}$$

The design resistance amounts to 256.1 kN, and the corresponding permanent load G_k is derived from Eq. (3) and equals 109.0 kN. Finally, the variable load Q_k is calculated using Eq. (4).

$$E_d = \gamma_G G_k + \gamma_Q Q_k = G_k \left(\gamma_G + \gamma_Q \frac{\chi}{1-\chi}\right) \tag{3}$$

$$Q_k = \frac{\chi}{1-\chi} G_k \tag{4}$$

Here, γ_G and γ_Q are partial factors for permanent and variable loads, respectively, as specified in the Eurocodes, and χ is the load ratio parameter considered to be 0.4 in this case study.

3.2 Probabilistic analysis

Latin Hypercube samples (LHS) are employed to account for the probabilistic nature of the variables. With LHS, a near-random sample of the probabilistic variables can be achieved while

covering the entire domain of the distribution with relatively few samples, in contrast with crude Monte Carlo samples. In this study, 100 simulations are executed to determine the resistance of the half-joint, both for the FEM calculation as for the STM calculation. As the STM concerns a series system, the capacity of the half-joint is considered to be the capacity of the weakest element in the model.

The corresponding failure probability $P_{f,}$ and reliability index β can be quantified by using the first-order reliability method (FORM). The following limit state equation is considered:

$$g(X) = K_R R - K_E (G + Q_{50}) \tag{5}$$

The corresponding failure probability of the element is approximately given by Eq. (6).

$$P_f = \Phi(-\beta) \tag{6}$$

4 RESULTS

In Figure 4 and Figure 5, the load-deflection curves of all the calculated samples are visualised by the grey lines. The corresponding 5% and 95% confidence intervals are shaded in blue. After reaching the peak load, i.e. at the moment when the rebars near the nib corner start to yield or when a critical shear crack starts to form, the samples reduce in capacity. Some fail due to the total rupture of the diagonal rebars, characterised by a steep drop in the load-deflection curve, while other simulations exhibit a more gradual decrease in capacity. The overall trajectory of the 3D and 2D graphs is similar, but there is a larger spread in the 2D model on the deflection corresponding to the moment of rupture of the diagonal bars, and the residual capacity at a deflection of 25 mm is smaller.

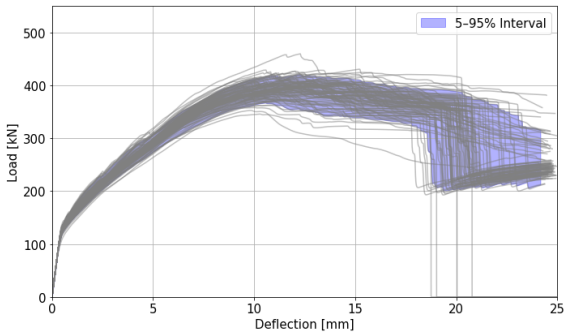

Figure 4: Load-deflection curve – 3D model

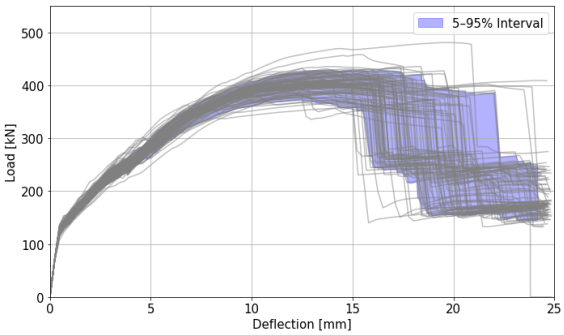

Figure 5: Load-deflection curve – 2D model

From the FEM simulations, performed with LHS, a distribution of the capacity of the half-joint can be achieved based on the peak load values of the different samples (see Figure 6 and Figure 7). The resistance distribution is approximated by a lognormal distribution. The distribution of the 3D FEM has a mean value of 397 kN and a standard deviation of 18.2 kN, while for the 2D FEM these values are 406 kN and 19.2 kN respectively. The calculated capacity of the half-joint is slightly smaller when using the 3D FEM and has a lower standard deviation compared to the 2D FEM.

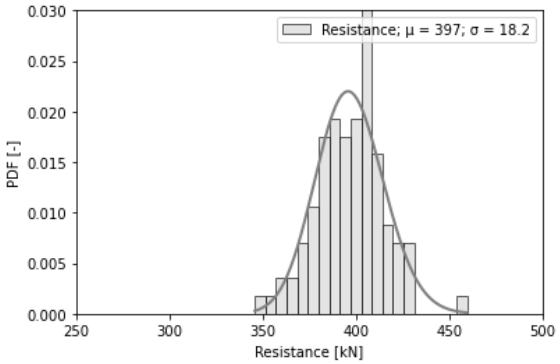

Figure 6: Resistance distribution – 3D model

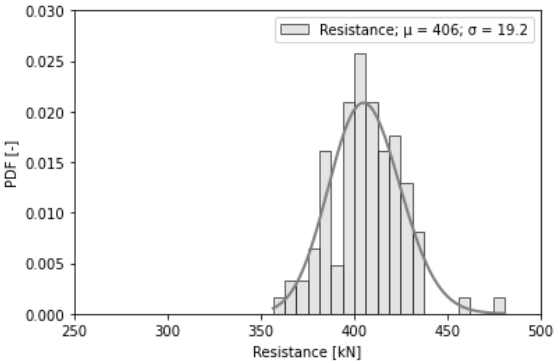

Figure 7: Resistance distribution– 2D model

With the same LHS as adopted for the FEM calculations, the STM and its corresponding capacity distribution are computed (see Figure 8). The resulting half-joint's capacity from the STM calculation can also be adequately described by a lognormal distribution, with a mean value of 334 kN and a standard deviation of 17.6 kN.

The distribution curves of the three different approaches are plotted in Figure 9 together with the distribution of the acting loads. It can be seen that the STM calculation yields a lower resistance for the studied half-joint in comparison with the 3D and 2D FEM, which could be expected, since it is a lower bound estimation of the actual capacity. It is nevertheless a relatively good approximation of the real behaviour of the half-joint, considering its very simple nature.

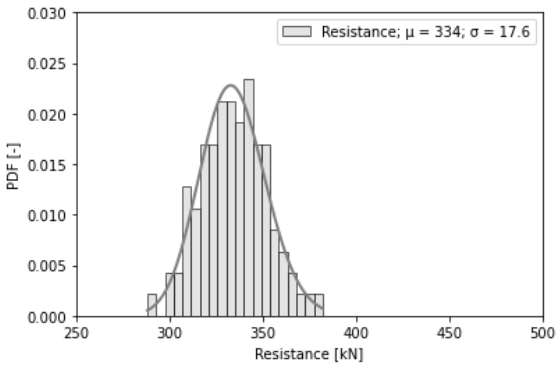

Figure 8: Resistance distribution – STM

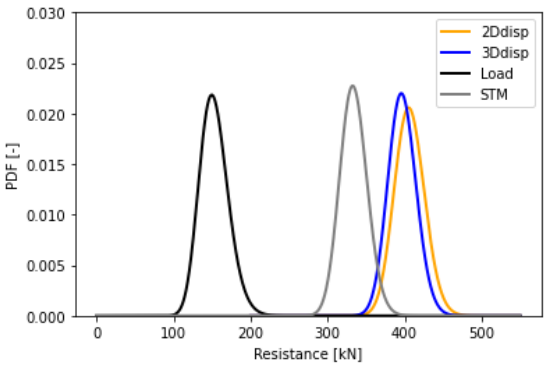

Figure 9: Load and resistance distributions

With the achieved lognormal distributions, representing the capacity of the half-joint based on the different calculation options (3D FEM, 2D FEM and STM), FORM analyses are executed using the limit state given in Eq. (5). In this equation, for the resistance R, the corresponding lognormal distribution is applied, while for the other parameters, the distributions and parameter values are listed in Table 1.

The resulting failure probabilities $P_{f,}$ and reliability indices β are given in Table 2. The values in the last row of the table are derived from a direct FORM analysis on the STM calculation without first approximating the resistance curve with a lognormal distribution. For this, the multivariate standard normal cumulative density function Φ_n is applied:

$$P_f \approx 1 - \Phi_n(\boldsymbol{\beta}; \boldsymbol{\rho}) \tag{7}$$

Where **β** is the vector of reliability indices of the different elements in the STM, and **ρ** is the covariance matrix, which is composed of correlation coefficients ρ_{ik}. For more information, reference is made to Luyten et al. [8].

Table 2: P_f and β of the different approaches

Model	P_f	β
3D Finite element model	$0.6069 \cdot 10^{-6}$	4.853
2D Finite element model	$0.3907 \cdot 10^{-6}$	4.940
STM – Calculated with LHS	$16.76 \cdot 10^{-6}$	4.148
STM – Calculated with direct FORM-analysis	$15.69 \cdot 10^{-6}$	4.163

The last two rows yield similar results, confirming that the approximation of the resistance curve based on LHS is a valid approach. Further, equivalent conclusions can be drawn as from Figure 9: the STM is a good lower bound approximation of the FEMs and hence of the real capacity of the half-joint. The design load was determined by a design calculation with the STM for a β_{target} equal to 3.8. The latter determines the partial factors for the loads (γ_G = 1.35 and γ_Q = 1.5) and the materials (γ_c = 1.5 and γ_s = 1.15). However, when calculating the capacity of the half-joint probabilistically, it appears that this initial design calculation involves an underestimation of the STM capacity, as the equated β-value equals approximately 4.15 to 4.94.

4.1 Failure mechanisms

In the analytical STM calculation, two types of failure occur. The first one is a failure of the diagonal rebars T_5, which occurs in 51% of the cases. The other 49% of the samples fail in tension tie T_2, which corresponds to the first two stirrups of the half-joint. Hence, all of the samples fail due to the yielding of the reinforcement. In the 3D FEM simulations, however, a different failure behaviour is noticed. This difference is possible due to the ability of a load redistribution in the FEM, while in the STM failure is immediately assumed when a tension tie reaches its yield strength as no strain hardening of the reinforcement is considered and the STM is an isostatic structure.

In all of the FEM samples the diagonal bars are the first to reach their yield strength, but in contrast to the STM this does not imply failure of the structure. Further, the compressive strength of the concrete has never been reached.

The first type of failure is failure at the re-entrant corner of the nib, covering 53% of the cases. In this failure mechanism, the yielding of the diagonal bars at the nib corner is followed by the yielding of the first stirrup at the same location. Subsequently, the U-bar also fails at this location when the load-deflection curves of these samples reach their maximum. An example of this failure mechanism is shown in Figure 10 and Figure 11. Generally, this failure type occurs when the steel strength is low in comparison to the concrete strength.

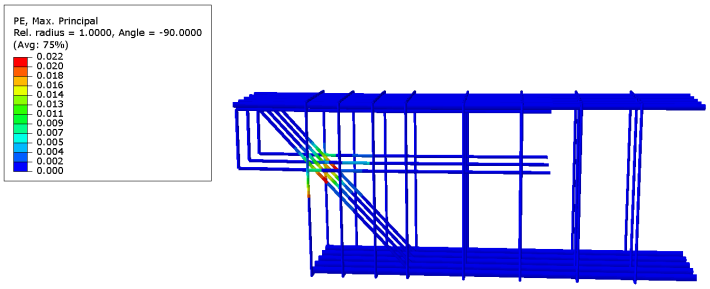

Figure 10: Plastic strains in the rebars – Nib failure

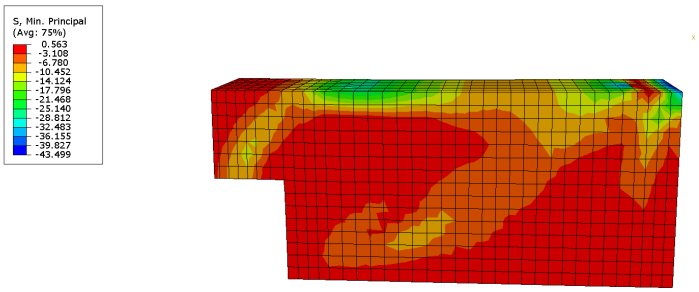

Figure 11: Compressive concrete stresses – Nib failure

A second failure mechanism is a shear crack failure, appearing more towards the midspan of the girder and originating from a bending crack. This crack then propagates along the bottom reinforcement towards the half-joint (see Figure 12). This second type occurs in 21% of the cases. It manifests itself by the yielding of one or more of the stirrups at midspan, followed by the yielding of the diagonal reinforcement close to the bottom rebars (see Figure 13 and Figure 14). This failure type generally occurs when the concrete strength is sufficiently low in comparison to the yield strength of the steel.

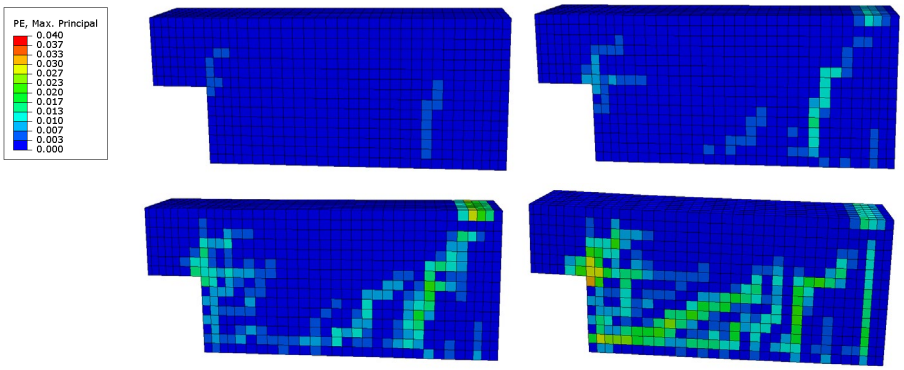

Figure 12: Evolution of shear crack failure

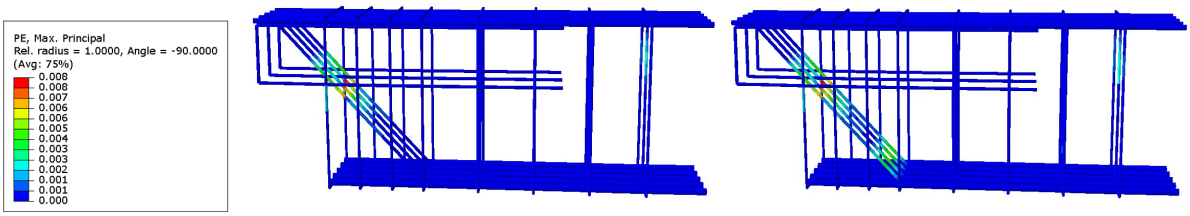

Figure 13: Plastic strains in the rebars – Shear crack failure (at peak load and just after)

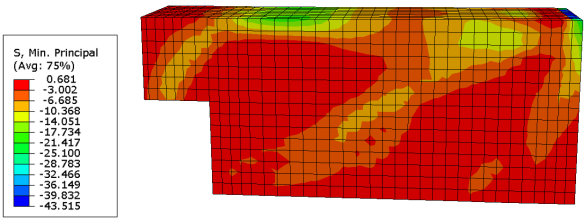

Figure 14: Compressive concrete stresses – Shear crack failure

Finally, a third failure mechanism that occurs is a combination of the previous two and covers 26% of the samples. It starts similarly to a shear crack, but there is not always significant yielding of the stirrups at midspan, nor of the diagonal rebars close to the bottom reinforcement. Afterwards, the failure state transitions to a failure at the nib corner.

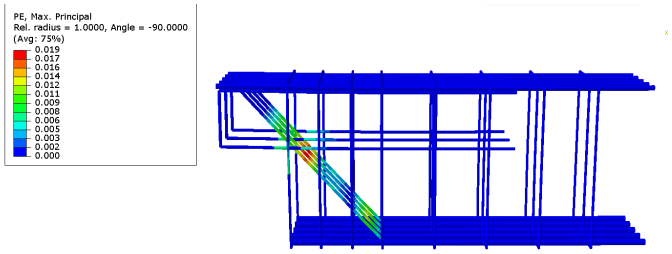

Figure 15: Plastic strains in the rebars – Combined failure

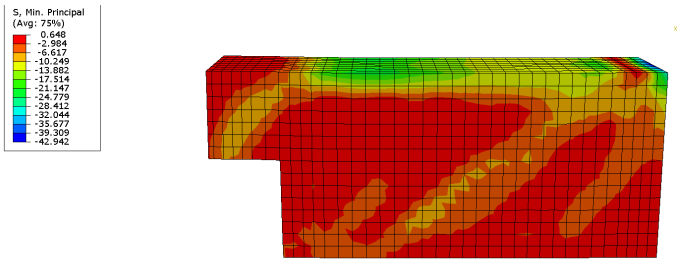

Figure 16: Compressive concrete stresses – Combined failure

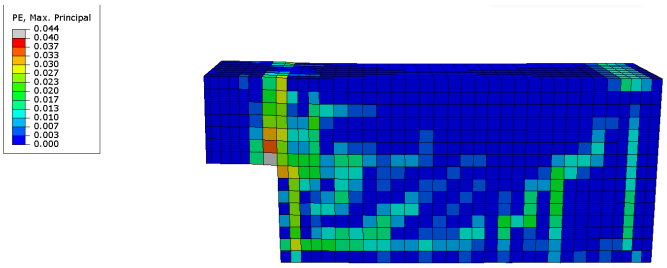

Figure 17: Final state of combined failure

5 CONCLUSIONS

This study investigated the structural reliability of concrete half-joints in discontinuity regions by comparing probabilistic results from strut-and-tie models (STMs) and finite element models (FEMs). The comparison enabled to assess the validity of lower bound STM approximations when compared with detailed 3D non-linear FEM simulations and simplified 2D non-linear FEM simulations under material and load uncertainties. It shows the importance of probabilistic FEM calculations in validating analytical models.

The developed 3D and 2D FEM accurately reproduced the experimental load-deflection response, validating its suitability as a numerical benchmark for evaluating other modelling strategies such as the STM. The peak load and overall structural behaviour matched the experimental results closely, with minor discrepancies that could be attributed to the fracture energy formulation.

The STM provided a conservative yet credible estimate of the half-joint's capacity. Probabilistic analysis confirmed that while the STM underestimates the capacity relative to the 3D FEM, the difference in mean resistance values (63 kN) remains acceptable for design purposes but can still be improved. Nevertheless, the STM yielded a reliability index $\beta = 4.15$, which exceeds the target value $\beta_{target} = 3.8$, indicating that for this case study the current design standards are overperforming in terms of safety margin on top of the inherent conservatism of the STM as the effective reliability index lies in the order of magnitude of 4.85 judging from the 3D FEM simulations. However, it might be that for a different geometry, a significantly lower reliability is achieved. Further research should be conducted to formulate a generally valid conclusion.

Despite the gain in computational efficiency offered by 2D models, a 3D finite element model remains essential for achieving accurate results, especially when assessing existing structures subjected to time-dependent degradation such as corrosion. Unlike 2D models with lumped out-of-plane reinforcement, 3D models allow for the individual modelling of each reinforcing bar. This enables a more detailed representation of phenomena like bond strength reduction and localised pitting corrosion.

Further, Latin Hypercube sampling (LHS) proves to be an efficient tool to account for the parameter uncertainties with a limited number of samples. This reduces the required calculation effort to obtain the resistance distribution with sufficient accuracy in its tails. The combination of LHS and the first-order reliability method (FORM) proved effective for evaluating structural reliability with a manageable number of FEM simulations. The approximation of the capacity distribution using LHS was validated by comparing results with a direct FORM analysis, confirming its appropriateness in probabilistic design.

Finally, the FEM simulations captured complex failure mechanisms that are not represented in the STM, particularly due to the FEM's ability to redistribute loads after local yielding. In the STM, failure follows immediately upon yielding of a tension tie, while the FEM showed an enhanced load-bearing capacity beyond initial yielding. Two dominant failure modes were observed in the FEM: one involving failure at the re-entrant corner of the nib and another through critical shear cracks.

Future work will focus on the improvement of the use of STMs for design purposes while reducing the inherent conservativeness.

ACKNOWLEDGEMENTS

This research was performed with support from FWO-Flanders (FWO Fellowship Fundamental Research - 11I8625N).

REFERENCES

[1] Desnerck, P., Lees, J. M., and Morley, C. T. Strut-and-tie models for deteriorated reinforced concrete half-joints. *Engineering Structures*. (2018) 161:41–54. doi:10.1016/j.engstruct.2018.01.013.

[2] Desnerck, P., Lees, J. M., and Morley, C. T. Impact of the reinforcement layout on the load capacity of reinforced concrete half-joints. *Engineering Structures*. (2016) 127:227–239. doi:10.1016/j.engstruct.2016.08.061.

[3] Passos Sério Lourenço, M. F., et al. Design and Assessment with Strut-and-Tie Models and Stress Fields: From Simple Calculations to Detailed Numerical Analysis. fib Bulletin 100. *The International Federation for Structural Concrete*. (2021). doi:10.35789/fib.BULL.0100.

[4] Luyten, K., Botte, W., and Caspeele, R. Probabilistic Quantification of the Structural Capacity in Concrete Discontinuity Regions Using Strut-and-Tie Models. 20th International Probabilistic Workshop. Edited by J. C. Matos et al. *Cham: Springer Nature Switzerland*. (2024) 494:429–439. doi:10.1007/978-3-031-60271-9_40.

[5] European Committee for Standardisation. EN 1992-1-1 Eurocode 2: Design of Concrete Structures - Part 1-1: General Rules and Rules for Buildings. *European Committee for Standardisation*. (2004).

[6] JCSS. Probabilistic model code. *Joint Committee on Structural Safety*. (2001). https://www.jcss-lc.org/jcss-probabilistic-model-code/.

[7] Caspeele, R., Sykora, M., and Taerwe, L. Influence of quality control of concrete on structural reliability: Assessment using a Bayesian approach. *Materials and Structures*. (2014) 47(1–2):105–116. doi:10.1617/s11527-013-0048-y.

[8] Luyten, K., Botte, W., and Caspeele, R. Towards a reliability-based design concept for concrete discontinuity regions using strut-and-tie models. fib symposium 2024 ReConStruct: Resilient Concrete Structures. 11-13 November 2024, Christchurch, New Zealand. *Proceedings fib symposium 2024*. (2024). 1455–1463. ISBN 978-2-940643-25-7